HYBRID DC ACCURATE CHARGE AMPLIFIER FOR LINEAR PIEZOELECTRIC POSITIONING

Andrew J. Fleming, S. O. Reza Moheimani

School of Electrical Engineering and Computer Science, University of Newcastle, Australia 2308

Abstract: Piezoelectric transducers are known to exhibit less hysterisis when driven with current or charge rather than voltage. Despite this advantage, such methods have found little practical application due to the poor low frequency response of present current and charge driver designs. This paper introduces a new circuit topology free from low-frequency drift and DC load offsets. The *hybrid load feedback charge amplifer* contains a secondary low-frequency voltage feedback loop to stabilize the low-frequency and DC operation of the amplifier.

Keywords: Charge, Amplifier, Driver, Source, DC, Piezoelectric, Load

1. INTRODUCTION

Piezoelectric transducers have found countless application in such fields as vibration control (Hagood *et al.*, 1990), nano-positioning (Croft *et al.*, 2000), acoustics (Niezrecki and Cudney, 2001), and sonar (Stansfield, 1991). The piezoelectric effect is a phenomena exhibited by certain materials where an applied electric field produces a corresponding strain and *vice versa* (Adriaens *et al.*, 2000) (*IEEE Standard on Piezoelectricity*, 1987) (Jaffe *et al.*, 1971). The effect can be exploited in one, two, or three dimensions, for actuating, sensing, or sensori-actuating (Dosch *et al.*, 1992).

One common theme across the diverse literature involving piezoelectric applications is the problem of hysteresis (Adriaens *et al.*, 2000) (Jaffe *et al.*, 1971). When used in an actuating role, piezoelectric transducers display a significant amount of hysteresis in the transfer function from voltage to displacement (Adriaens *et al.*, 2000) (Jaffe *et al.*, 1971).

As discussed in (Furutani *et al.*, 1998) and references therein, a great number of techniques have been developed with the intention of reducing hysteresis. Included are: displacement feedback techniques, mathematical Preisach modeling (Mayergoyz, 1991) and inversion, phase control, polynomial approximation, and current or charge actuation (Newcomb and Flinn, 1982).

Almost all contributions in this area make reference to the well known advantages of driving piezoelectric transducers with current or charge rather than voltage (Newcomb and Flinn, 1982). Simply by regulating the current or charge, a five-fold reduction in the hysteresis can be achieved (Ge and Jouaneh, 1996). A quote from a recent paper (Cruz-Hernandez and Hayward, 2001) typifies the sentiment towards this technique:

> "While hysteresis in a piezoelectric actuator is reduced if the charge is regulated instead of the voltage (Newcomb and Flinn, 1982), the implementation complexity of this technique prevents a wide acceptance (Kaizuka and Siu, 1988)".

Although the circuit topology of a charge or current amplifier is much the same as a simple voltage feedback amplifier, the uncontrolled nature of the output voltage typically results in the load capacitor being charged up. Saturation and distortion occur when the output voltage, referred to as the compliance voltage, reaches the power supply rails. The stated *complexity*

[1] This work was supported by the Australian Research Council.

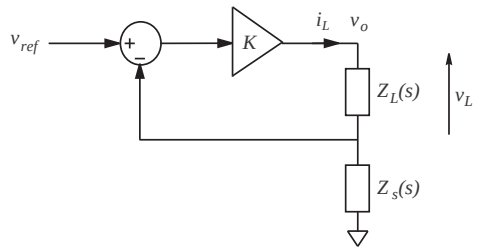

Fig. 1. A generic charge driver, where the load and sensing impedance is represented by $Z_L(s)$ and $Z_s(s)$ respectively.

invariably refers to the need for additional circuitry to avoid charging of the load capacitor. A popular technique is to simply short circuit the load every $400\ ms$ or so, periodically discharging the load capacitance and returning the DC compliance voltage to ground (Main *et al.*, 1995) (Comstock, 1981). This introduces undesirable high frequency disturbance and severely distorts low frequency charge signals.

This paper presents a new class of charge amplifier free from DC and low-frequency voltage drift. In the following section, the design of basic charge amplifiers and their associated problems are discussed. As an alternative, the *hybrid voltage feedback charge amplifier* is introduced in section 3. Experimental implementation and results are presented in section 4. The paper is concluded with a summary and discussion in section 5.

2. BASIC CIRCUIT CONFIGURATIONS

Consider the simplified diagram of a generic current source shown in Figure 1. The high gain feedback loop and voltage driver works to equate the applied reference voltage v_{ref}, to the sensing voltage v_s. In the Laplace domain, at frequencies well within the bandwidth of the control loop, the load current $I_L(s)$ is equal to $V_{ref}(s)/Z_s(s)$.

If $Z_s(s)$ is a capacitor C_s,

$$\dot{q}_L = I_L(s) = V_{ref}(s)C_s s, \tag{1}$$

$$q_L = V_{ref}(s)C_s, \tag{2}$$

i.e. we have a charge amplifier with gain $C_s\ Columbs/V$.

As mentioned in the introduction, the foremost difficulty in employing such devices to drive highly capacitive loads is that of DC current or charge offsets. Inevitably, the voltage measured across the sensing impedance will contain a non-zero voltage offset, this and other sources of voltage or current offset within the circuit result in a net output current offset. As a capacitor integrates DC current, the uncontrolled output voltage will ramp upward and saturate at the power supply rail. Any offset in v_o limits the compliance range of the current source and may eventually cause saturation. To limit the DC impedance of a capacitive load (i.e. $Z_L(s) = \frac{1}{C_L s}$), a parallel resistance is often used. In this case, the load impedance $Z_L(s)$ is equal to the parallel combination of the load capacitance C_L and the compensation resistor R_L. The actual charge $q_{Lc}(s)$ flowing through the load capacitor becomes

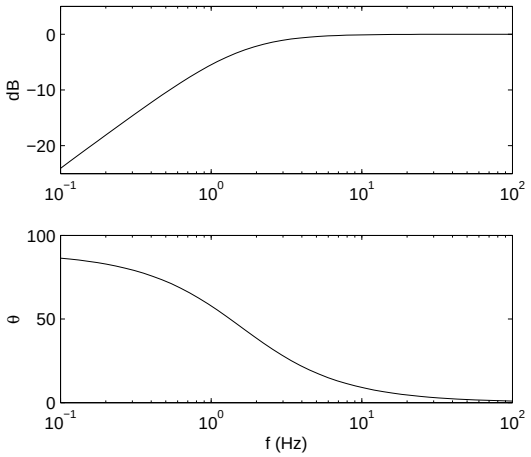

Fig. 2. Typical frequency response from an applied reference voltage to the actual capacitive load current $I_{Lc}(s)$.

$$q_{Lc}(s) = q_L(s)\frac{s}{s + \frac{1}{R_L C_L}}. \tag{3}$$

Additional dynamics have been added to the charge source. The transfer function now contains a high-pass filter with cutoff $\omega_c = \frac{1}{R_L C_L}$. That is,

$$\frac{q_{Lc}(s)}{V_{ref}(s)} = C_s\frac{s}{s + \frac{1}{R_L C_L}}. \tag{4}$$

In contrast to the infinite DC impedance of a purely capacitive load, the load impedance now approaches R_L at frequencies below $\omega_c = \frac{1}{R_L C_L}$. Thus, a DC offset current of i_{dc} results in a compliance voltage offset of $v_o = i_{dc}R_L$. In a typical piezoelectric drive scenario, with $C_L = 100\ \eta F$, and $i_{dc} = 1\mu A$, a $1\ M\Omega$ parallel resistance is required to limit the DC compliance offset to $1\ V$. The frequency response from an applied reference voltage to the actual capacitive load current $i_{Lc}(s)$ is shown in Figure 2. Phase lead exceeds 5 degrees below $18\ Hz$. Such poor low frequency performance precludes the use of current amplifiers in applications requiring accurate low frequency tracking, e.g. Atomic Force Microscopy (Croft *et al.*, 2000). The advantages of piezoelectric current excitation are lost to the practical electronic difficulties in constructing a charge source.

The following section introduces a new type of charge source, the *hybrid voltage feedback charge amplifier* corrects for any DC or low-frequency infidelity.

3. HYBRID VOLTAGE FEEDBACK

Figure 3 shows the schematic diagram of a hybrid voltage feedback charge amplifier. Neglecting the shaded voltage feedback componentry, the circuit is

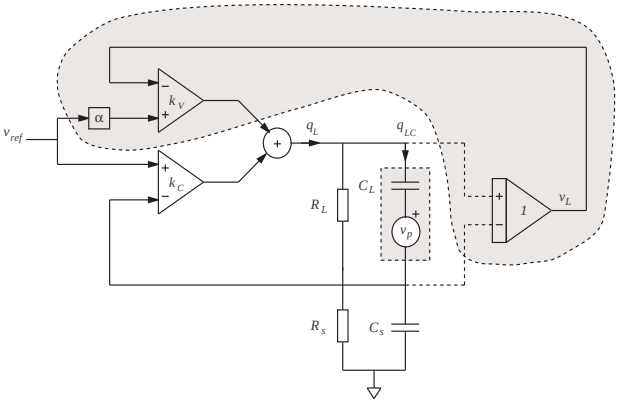

Fig. 3. Simplified schematic of a voltage feedback charge amplifier. Respectively, k_V and k_C are the voltage and charge feedback controllers.

simply a realization of the diagram shown in Figure 1. Charge q_c is supplied to the piezoelectric load modeled as a voltage source v_p in series with a capacitor C_L. The parallel load resistance R_L is included to model finite buffer impedance and transducer dielectric leakage. Charge sensing is performed by the capacitance C_s and parallel resistance R_s. The resistor R_s provides a path for bias currents and DC current generated from constant load voltages. The magnitude of R_s is prescribed by R_L and the amount of DC current associated with the instrumentation electronics.

The objective is to supply a load charge q_{LC} directly proportional to the reference voltage v_{ref}. As discussed in the previous section, the foremost difficulty precluding such operation is the presence of a parallel load resistance R_L. At low frequencies and DC, charge is effectively bled through this resistor. In addition, the presence of a parallel sensing resistance R_s renders the charge amplifier as a current source at low frequencies and DC. Although both of these resistors are necessary for practical circuit operation, the amplifier is incapable of correct low-frequency and DC operation.

This paper proposes hybrid load voltage feedback as a technique for correcting the low-frequency dynamics of a charge amplifier. Consider the shaded circuit area shown in Figure 3, the voltage feedback mechanism comprises a controller k_V, load voltage measurement v_L, and set-point αv_{ref}. This topology is based on the observation that voltage drop across a purely capacitive load is proportional to the charge q_{LC}. Where the charge amplifier has a gain of C_s C/V, the expected load voltage drop is $\frac{v_{ref}C_s}{C_L}$. The voltage feedback loop is simply designed to enforce this relationship at low-frequencies and DC. Hence the selection of $\alpha = C_s/C_L$.

Effectively the circuit contains two additive amplifiers, a genuine charge amplifier over medium and high frequencies, and a voltage amplifier synthesizing the operation of an ideal charge amplifier at low-

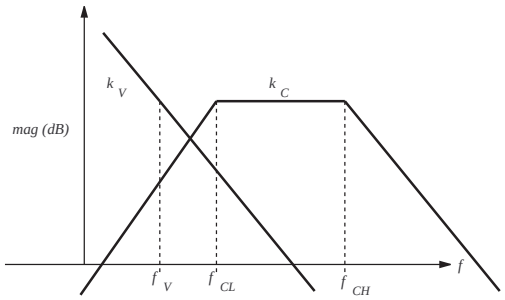

Fig. 4. Simple controller choices for k_V and k_C.

frequencies and DC. The two design objectives are as follows:

- The charge applied to a capacitive load should be proportional to the reference voltage. i.e. the transfer function from an applied reference voltage v_{ref} to the actual load charge q_{LC}, expressed as $\frac{q_{LC}(s)}{C_s v_{ref}(s)}$ should equal 1. For capacitive loads, the equivalent transfer function $\frac{v_L(s)}{v_{ref}(s)}$ is easier to measure experimentally. This transfer function will be referred to as the tracking performance. Ideal tracking performance is identified by $\frac{v_L(j\omega)}{v_{ref}(j\omega)} = 1, \forall\, \omega$.
- Piezoelectric loads are not purely capacitive, they also contain resistance and an internal voltage source. Within the frequency range where the voltage feedback loop is dominant, such additional dynamics add to the voltage drop and introduce errors in q_{LC}. For the purpose of differentiating between voltage-synthesis and pure-charge driven operation, we consider the transfer function $\frac{v_L(s)}{v_p(s)}$. Within a frequency range where $\frac{v_L(j\omega)}{v_p(j\omega)} = 1$, the circuit is operating purely as a charge amplifier. Obviously our objective is to obtain this mode of operation over as wide a frequency band as possible.

Based on Figure 3, the two transfer functions of interest $\frac{v_L(s)}{v_{ref}(s)}$ and $\frac{v_L(s)}{v_p(s)}$ can be derived as follows:

$$\frac{v_L(s)}{v_{ref}(s)} = \frac{R_L\left(k_C + \alpha k_V\right)}{sR_LC_LZ_s\left(1+k_C\right) + R_L + Z_s + Z_sk_C + R_Lk_V}, \quad (5)$$

$$\frac{v_L(s)}{v_p(s)} = \frac{R_L}{\beta + R_Lk_V}\frac{sC_LZ_s\beta + Z_sR_LC_Lk_C}{R_L + Z_s + sR_LC_LZ_s} \quad (6)$$

where Z_s, the sensing impedance, is equal to $\frac{R_s}{1+sR_sC_s}$, $\alpha = C_s/C_L$, and $\beta = (R_L + Z_s + sR_LC_LZ_s + Z_sk_C + sR_LC_LZ_sk_C)$.

Simple control design principles can be applied to obtain suitable controllers for k_V and k_C:

- To minimize tracking error, the combination of both control loops should apply a high feedback gain over the entire amplifier bandwidth.

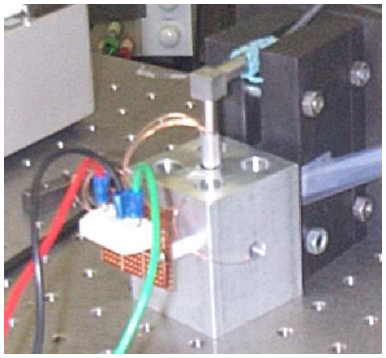

Fig. 5. The piezoelectric tube apparatus. In this experiment, the capacitive sensor (facing the back side of the tube top) and the tube cap are not used.

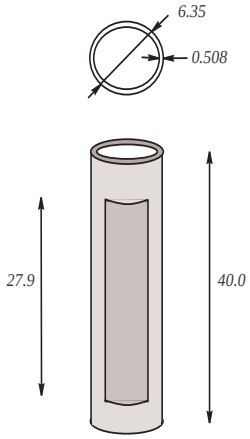

Fig. 6. Piezoelectric tube dimensions (all measurements in mm).

- The individual bandwidths of each loop should be mutually exclusive, i.e. they should not interfere with one another.

Given these guidelines, simple and easy-to-implement choices for k_V and k_C are shown in Figure 4. The voltage controller k_V is an integrator that applies large control effort at frequencies below f_V. The charge controller k_C contains a high-pass filter to avoid interference with k_V, and a low-pass filter to roll-off the amplifier gain at high-frequencies. The in-bandwidth feedback gain of k_C will be referred to as λ. First-order transfer function representations of the two controllers are shown below,

$$k_C = \lambda \frac{s}{s + 2\pi f_{CL}} \frac{2\pi f_{CH}}{s + 2\pi f_{CH}} \tag{7}$$

$$k_V = \lambda \frac{2\pi f_V}{s}. \tag{8}$$

4. EXPERIMENTAL RESULTS

In this section a prototype amplifier is employed to drive a piezoelectric tube positioner in one dimension. The apparatus and corresponding dimensions are shown in Figures 5 and 6.

R_L	$165\ M\Omega$
C_L	$8\ nF$
R_s	$99\ M\Omega$
C_L	$100\ nF$

Table 1. Characteristics of the load and sensing impedance.

f_V	$1\ Hz$
$f_{CL,}$	$10\ Hz$
f_{CH}	$500\ Hz$
λ	2000

Table 2. Controller parameters.

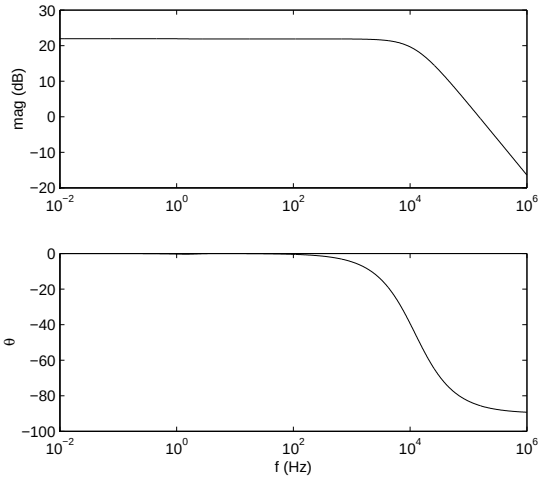

Fig. 7. The tracking performance $\frac{v_L(s)}{v_{ref}(s)}$.

The electrical characteristics of the load and sensing impedance are shown in Table 1. Suitable values of f_V, $f_{CL,}$ and f_{CH} are shown in Table 2. The resulting tracking performance and charge-voltage sharing is shown in Figures 7 and 8. From these responses it can be concluded that the amplifier is capable of maintaining DC charge references, has negligible in-bandwidth gain ripple, and operates dominantly in charge mode above a frequency of 2 Hz.

To verify the amplifiers operation, an approximately ± 7 micron ramped sinusoidal displacement was generated by the piezoelectric tube. This magnitude of travel required a peak field of approximately $\pm 240\ \frac{V}{mm}$. A Polytec laser vibrometer was employed to measure the displacement of the tip. The voltage and charge responses are shown in Figures 9 and 10. As expected, the charge driven response displays a significantly lesser hysteresis.

5. CONCLUSIONS

A new charge amplifier topology has been presented to correct the poor low-frequency tracking performance of current circuit designs. The *hybrid voltage feedback charge amplifier* synthesizes the operation of an ideal charge amplifier at frequencies where the primary charge feedback loop is ineffective, inaccurate, or unstable.

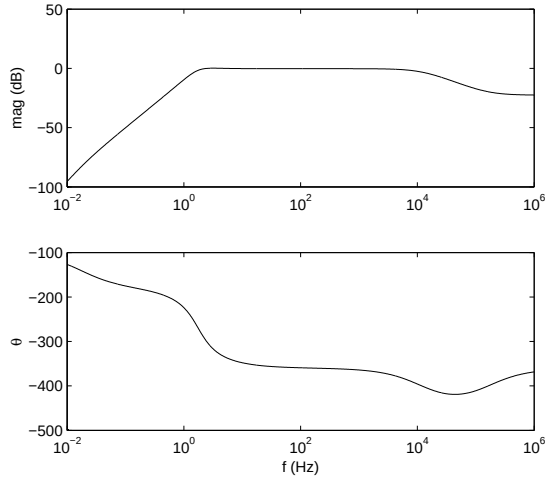

Fig. 8. The voltage-charge sharing $\frac{v_L(s)}{v_p(s)}$.

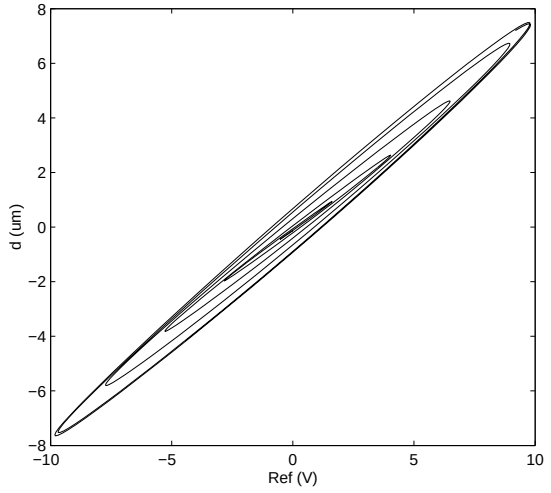

Fig. 9. Voltage driven tube response to a ramped 100 Hz sinusoid.

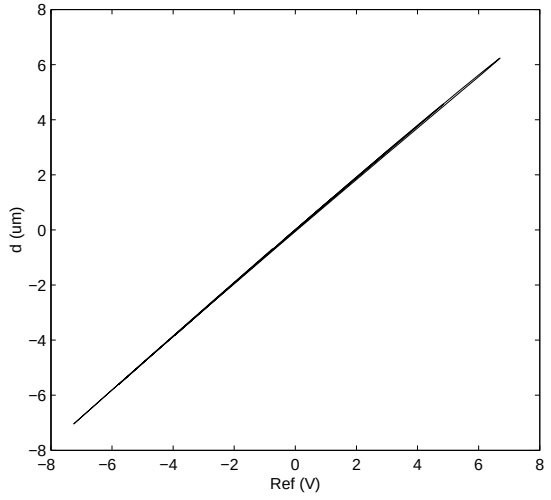

Fig. 10. Charge driven tube response to a ramped 100 Hz sinusoid.

An experimental amplifier connected to an 8 nF piezoelectric load demonstrated excellent charge tracking with dominant charge operation above 2 Hz.

6. REFERENCES

Adriaens, H. J. M. T. A., W. L. de Koning and R. Banning (2000). Modeling piezoelectric actuators. *IEEE/ASME transactions on mechatronics* **5**(4), 331–341.

Comstock, R. (1981). Charge control of piezoelectric actuators to reduce hysteresis effects. *Japan Journal of Applied Physics, part 2 - Letters*.

Croft, D., G. Shedd and S. Devasia (2000). Creep, hysteresis and vibration compensation for piezoactuators: Atomic force microscopy application. In: *Proc. American Control Conference*. Chicago, Illinois. pp. 2123–2128.

Cruz-Hernandez, J. M. and V. Hayward (2001). Phase control approach to hysteresis reduction. *IEEE transactions on control systems technology* **9**(1), 17–26.

Dosch, J. J., D. J. Inman and E. Garcia (1992). A self-sensing piezoelectric actuator for collocated control. *Journal of Intelligent Material Systems and Structures* **3**, 166–185.

Furutani, K., M. Urushibata and N. Mohri (1998). Improvement of control method for piezoelectric actuator by combining charge feedback with inverse transfer function compensation.. In: *Proc. IEEE International Conference on Robotics and Automation*. Leuven, Belgium. pp. 1504–1509.

Ge, P. and M. Jouaneh (1996). Tracking control of a piezoelectric actuator. *IEEE Transactions on control systems technology* **4**(3), 209–216.

Hagood, N. W., W. H. Chung and A. von Flotow (1990). Modelling of piezoelectric actuator dynamics for active structural control. *Journal of Intelligent Material Systems and Structures* **1**, 327–354.

IEEE Standard on Piezoelectricity (1987). ANSI/IEEE standard 176-1987.

Jaffe, B., W. R. Cook and H. Jaffe (1971). *Piezoelectric Ceramics*. Academic Press. St. Louis, MO.

Kaizuka, H. and B. Siu (1988). Simple way to reduce hysteresis and creep when using piezoelectric actuators. *Japan Journal of Applied Physics, part 2 - Letters* **27**(5), 773–776.

Main, J. A., E. Garcia and D. V. Newton (1995). Precision position control of piezoelectric actuators using charge feedback. *Journal of Guidance, control, and dynamics* **18**(5), 1068–1073.

Mayergoyz, I. D. (1991). *Mathematical Models of Hysteresis*. Springer Verlag. New York.

Newcomb, C. V. and I. Flinn (1982). Improving the linearity of piezoelectric ceramic actuators. *IEE Electronics Letters* **18**(11), 442–443.

Niezrecki, C. and H. H. Cudney (2001). Feasibility to control launch vehicle internal acoustics using

piezoelectric actuators. *Journal of Intelligent Material Systems and Structures* **12**, 647–660.

Stansfield, D. (1991). *Underwater Electroacoustic Transducers*. Bath University Press and Institute of Acoustics. Bath, UK.